The Gibraltar strait system controls the exchange between the Mediterranean basin and the global ocean. In this region, large topographic variations and strong tidal currents (up to 1.8 m/s above Camarinal sill) lead to complex generation mechanisms of energetic non-linear internal waves (Vázquez et al., 2006; Vlasenko et al., 2009). The propagation of these waves is highly influenced by the complex basin geometry (Sánchez-Garrido et al., 2011) and the hydraulic criticality of the flow (Sannino, 2009; Sannino et al., 2007). These local fine scale processes are driving turbulence levels in the order of magnitude larger than open-ocean levels (Wesson and Gregg, 1994) possibly affecting water-mass exchange (Sannino et al., 2015). The interplays of these processes with the vertical mixing and local circulation are still an ongoing scientific issue. A non-hydrostatic and non-Boussinesq model (the CROCO ocean community model) has been implemented in a realistic 3D configuration on the strait of Gibraltar area to model explicitly these fine scale processes. The 3D high resolution (200m) model is forced by the main barotropic tidal components (i.e. M2, S2, K1, O1) through the specification of the ENEA Mediterranean-Black Sea tidal operative forecasting system solutions. It provides a good representation of the barotropic & baroclinic tides in the strait of Gibraltar, representing well the internal fine-scale activity: hydraulic jumps formation above the main sills, internal solitary wave's generation & propagation, neap-spring tide variability...

0.0.1 The modeling approach

0.0.1.1 The model

Simulations are performed using the free-surface nonhydrostatic and non-Boussinesq version of the coastal and regional ocean community model CROCO. CROCO is a new oceanic modeling system built upon ROMS_AGRIF and the non-hydrostatic kernel of SNH. It solves the dynamic and thermodynamic equations using stretched, terrain-following vertical s-coordinates and orthogonal, curvilinear horizontal coordinates with a time-splitting between baroclinic and barotropic modes. For general circulation purposes, it is forced by atmospheric momentum, heat and tracer fluxes. For a more extensive description and technical details of the hydrodynamic model as well as earlier applications to the US West Coast, we refer to Shchepetkin and McWilliams (1998, 2003, 2005), Marchesiello et al. (2001, 2003) and to Penven et al. (2006).

The nonhydrostatic and non-Boussinesq version of CROCO uses an original two-mode time-splitting technique between barotropic ($\Delta\ t_e$
) and non-hydrostatic ($\Delta\ t_{NBQ}$
) motions to deal with free surface, non-hydrostatic flows and acoustic waves which are explicitly simulated. In the present non-Boussinesq version, a time-splitting is performed to circumvent the drastic CFL criteria induced by the high phase-velocity of such waves, c_s
. Acoustic waves or more exactly "pseudo-acoustic" waves have indeed been re-introduced to reduce computational costs. Indeed, this allows to avoid Boussinesq- degeneracy which inevitably leads to a 3D Poisson-system in non-hydrostatic pressure-correction methods. As long as they remain faster than the fastest physical processes in the domain, the so-called "pseudo-acoustic" wave phase-velocity can artificially be slowed down rendering unphysical high-frequency processes associated with bulk compressibility but preserving a coherent slow dynamics with a softening of the CFL criterion.

To model explicitly internal fine-scale turbulent processes in Gibraltar strait, we adopt a Monotone-Integrated Large Eddy Simulation
(MILES) approach. In MILES, the dissipative nature of some classes of advection schemes is exploited to provide an implicit model of turbulence. Small values of the kinematic viscosity (ν = 10e-6 m2/s) and density diffusivity (Kρ = 10e-6 m2/s) are used, without neither turbulence closure scheme nor additional viscosity (visc2=0). Numerical dissipation is provided through a Total Variation Diminishing (TVD) advection scheme for the momentum and a fifth-order WENO advection scheme for the tracers. TVD and WENO5 schemes are modern shock-capturing schemes which allow the capture of sharp discontinuities. The objective is not to reproduce the entire turbulent cascade but to be able, from this kind of simulation, to resolve explicitly the largest features of the internal fines-scale turbulent processes.

0.0.1.2 The numerical configurations

A non-hydrostatic (R_{NBQ}) and a hydrostatic (R_H) simulation are performed. A 3D version of the model is used with lateral Orlanski radiation condition, free surface boundary conditions and free-slip condition at the bottom. A constant quadratic bottom stress formulation is used with a drag coefficient of 10^{-3}. The model domain extends from the Gulf of Cadiz to the Alboran sea (Figure 1). The horizontal grid is kept constant at the resolution of 220 m and the vertical model grid is based on 40 sigma levels. Initial conditions for temperature and salinity were obtained from the ENEA Mediterranean-Black Sea tidal operative forecasting system[1]. Wind and surface fluxes are not included in the simulations. Tides are incorporated in the model through the specification at the lateral boundary of the barotropic velocity and the surface elevation obtained from the ENEA Mediterranean-Black Sea tidal operative forecasting system. The ENEA forecasting system provides also lateral boundary conditions in terms of salinity, temperature and baroclinic velocities (geostrophic currents). Table 1 summarizes the numerical and physical parameters of both configurations.

[1] * * *

	R_{NBQ}
(Nx, Ny, Nz, Nt)	(408, 523, 40, 669 600)
t	[10/09/2017 – 10/10/2017]
(Δ x, Δ y, Δ z)	(220 m, 220 m, 7-23 m)
(Δ t, N_e)	(4s, 9)
Cs	400 m/s
Bathymetry	SHOM (500 m)
Tidal forcing	ENEA Mediterranean-Black Sea tidal operative forecasting system
	M2, S2, K1, O1
Stratification	ENEA Mediterranean-Black Sea tidal operative forecasting system
Geostrophic currents	ENEA Mediterranean-Black Sea tidal operative forecasting system
Atmospheric forcing	No
Advection schemes	TVD (U-V-W) & WENO5 (T-S)

Table 1: Numerical & physical parameters of the non-hydrostatic run $\boldsymbol{R_{NBQ}}$.

The depth data were obtained from a 500 m resolution topographic data set of the Strait of Gibraltar provided from the SHOM (HOMONIM 500 m Grid). A Gaussian interpolation of the topography data has been made (rmax=0.25, hmin=30m) to set up the 220m-grid. The resulting model bathymetry is illustrated on figure 1a. On the vertical section of figure 1b, the dominant topographic features of the strait are clearly recognizable (from west to east): Espartel sill (ES); Tangier basin (TB); Camarinal sill (CS), with the minimum depth of 188 m, and Tarifa Narrows (TN) with the maximum depth of 960 m. This vertical section (located by the black line on figure 1a) has been selected to incorporate ES, the shallowest point of CS and the deepest point of TN. The vertical resolution (dz = 7-23 m) is much higher above Camarinal sill than in the eastern and western ends.

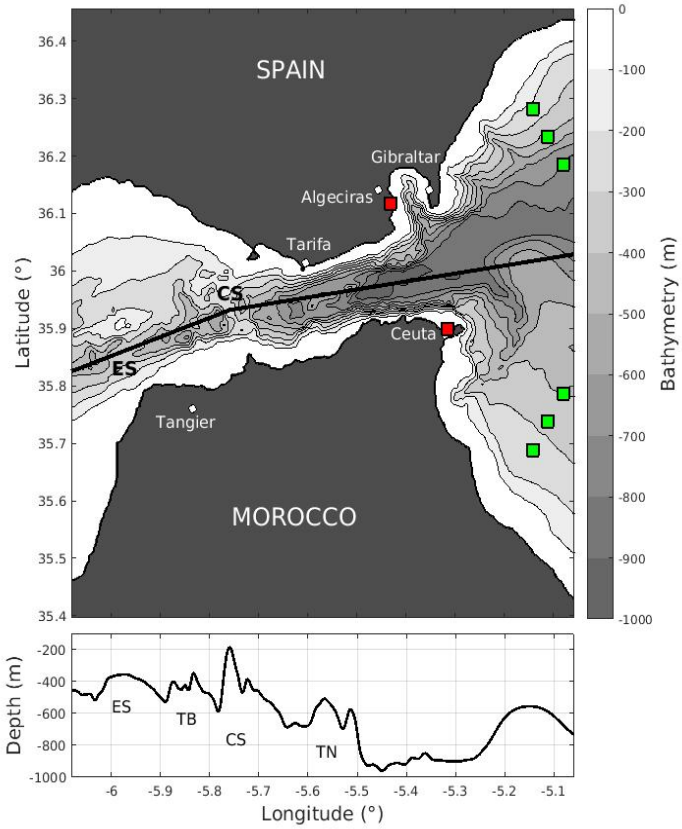

Figure 1: Bathymetry and domain extension of R_{NBQ} & R_H. The black line locate the vertical transect/section on the lower plot. Red squares locate tidal gauges position and green squares locate Xtrack position.

0.0.2 The Barotropic tides

Simulation		R_{NBQ}				R_H			
		dA (cm)	dG (°)	| | dE| | (cm)	| | **dE**| | /**A** (%)	dA (cm)	dG (°)	| | dE| | (cm)	| | **dE**| | /**A** (%)
M2	North	4.8+-0.7	0.7+-3.6	3.4+-1.2	**15.3**	4.8+-0.7	0.3+-3.6	3.4+-1.2	**15.3**
	South	4.5+-0.7	-10.6+-4.4	4.3+-1.4	**19.5**	4.4+-0.7	-11.1+-4.4	4.4+-1.5	**19.6**
S2	North	0.1+-2	11.3+-16	0.9+-2	**24**	0.2+-1.8	11.3+-16	0.8+-1.9	**23.5**
	South	1.2+-0.9	-5.5+-3	1+-0.7	**14.1**	1.2+1.0	-6.0+-3	1+-0.7	**14.3**
K1	North	-0.01+-0.1	2.2+-1.8	0.1+-0.7	**20.4**	-0.02+-1.0	0.8+-1.1	0.1+-0.7	**21.1**
	South	-1.7+-0.8	37.8+-2.5	1.6+-0.5	**66.5**	-1.5+-0.8	37.8+-2.3	1.6+-0.5	**65.4**
O1	North	-0.8+-0.6	-10.7± 13.6	0.7+-0.5	**46.6**	-1+-0.6	-8.1± 13.0	0.8+-0.5	**48.8**
	South	0.2+-0.5	-8.5+-18.5	0.2+-0.7	**25.6**	0.09+-0.5	-5.7+-18.6	0.1+-0.7	**25.3**

0.0.2.0.1 Comparison to X-track altimetry *Table 2 : Model performance statistics for the main barotropic tidal components (M2, S2, K1, O1) in* $\boldsymbol{R_{NBQ}}$ & $\boldsymbol{R_H}$ *and the forcing simulation in comparison to X-TRACK altimetry. dA = mean amplitude biais; dG = mean phase bias;* | | *dE*| | *= mean combined bias;* | | *dE*| | */A = mean relative bias.*

Simulation		Forcing (MITgcm)				TPX08			
		dA (cm)	dG (°)	| | dE| | (cm)	| | **dE**| | /**A** (%)	dA (cm)	dG (°)	| | dE| | (cm)	| | **dE**| | /**A** (%)
M2	North	4.8 ± 0.6	9.1 ± 3.3	4.2± 1.1	**18.5**	0.9 ± 0.4	0.7± 3.6	0.6± 1.2	**4.8**
	South	5.6± 0.7	0.5± 4.7	3.9± 1.5	**19.0**	0.3± 0.9	-3.6± 4.5	1.2± 1.5	**6.1**
S2	North	0.3± 1.8	17.5± 15.4	1.4± 1.9	**27.5**	-1.0± 1.8	12.3± 15.4	1.3± 1.9	**19.4**
	South	-1.2± 0.1	21.1± 10.5	1.0± 0.6	**13.6**	-0.2± 1.0	-3.9± 2.4	0.4± 0.8	**9.2**
K1	North	0.4 ± 1.0	8.7 ± 1.3	0.5± 0.7	**25.9**	0.5 ± 0.9	14.0 ± 2.6	0.7± 0.7	**28.7**
	South	-1.1± 0.8	44.0± 2.4	1.4± 0.6	**66.4**	-1.7± 0.8	59.8± 3.2	2.2± 0.5	**84.4**
O1	North	-0.2± 0.5	-15.8± 13	0.4± 0.5	**35.2**	0.01± 0.5	-3.1± 14.1	0.1± 0.4	**29.1**
	South	0.7± 0.4	-28.3± 23	0.8± 0.7	**44.3**	1.1± 0.4	30.7± 16.5	1.0± 0.6	**53.5**

=> Asymétrie Nord-Sud : Meilleure score de CROCO au Nord, meilleure score du MITgcm dans le su

=> Globalement semi-diurne bien mieux représentées que diurnes dans les 3 simulations.
Mais les Diurnes sont également mal représentées dans les modèles avec assimilation de des diurnes
données. Exemple TPX08 mauvaise représentation

=> Mauvaise représentation des diurnes = Problème connu! (∗ ∗ Ref?∗ ∗).

Simulation	R_{NBQ}				Forcing (MITgcm)			
	dA (cm)	dG (°)	| | dE| | (cm)	| | **dE**| | /**A** (%)	dA (cm)	dG (°)	| | dE| | (cm)	| | **dE**| | /**A** (%)
M2	3.9 ± 0.4	-1.6 ± 1.5	2.8± 0.5	**9.8**	-4.5± 0.5	4.6± 1.0	3.6± 0.5	**12.7**
S2	0.6± 0.3	-1.5± 0.9	0.5± 0.2	**4.7**	1.1± 0.3	2.8± 0.6	0.9± 0.2	**8.4**
K1	-1.3± 0.6	-5.1± 0.1	0.9± 0.4	**24.2**	-1.0± 0.3	0.2± 0.0	0.7± 0.2	**20.6**
O1	-1.2± 0.1	21.1± 10.5	1.0± 0.6	**47.5**	-0.7± 0.6	16.6± 8.1	0.6± 0.4	**33.5**

0.0.2.0.2 Comparison to tidal gauges *Table 3 : Model performance statistics for the main barotropic tidal components (M2, S2, K1, O1) in* $\boldsymbol{R_{NBQ}}$ & $\boldsymbol{R_H}$ *and the forcing simulation in comparison to tidal gauges. dA = mean amplitude biais; dG = mean phase bias;* $||dE||$ *= mean combined bias;* $||dE||/A$ *= mean relative bias.*

Simulation		R_{NBQ}				Forcing			
Tidal compo-nents	Tidal gauges	dA (cm)	dG (°)	| | dE| | (cm)	| | **dE**| | /**A** (%)	dA (cm)	dG (°)	| | dE| | (cm)	| | **dE**| | /**A** (%)
M2	Algeciras	-3.8	-2	4.0	**12.5**	-3.7	-8	5.5	**17.2**
	Ceuta	-4.4	3	4.7	**15.7**	-5.1	-3	5.4	**18**
	Gibraltar	-6.5	0	6.5	**20.3**	-6	-8	7.3	**22.8**
	Tarifa	-5.6	-1	5.7	**13.6**	-6.4	-2	6.6	**15.7**
	Mean	5.1± 1.0	0.1± 2.1	3.6± 1.0	**11.8**	-5.3± 1.1	5.2± 2.7	4.2± 1.3	**14.0**
S2	Algeciras	-0.14	1	0.3	**2.5**	-0.66	-5	1.2	**10.0**
	Ceuta	-0.95	1	1.0	**9.1**	-1.5	-2	1.5	**13.6**

continued on next page

continued from previous page

	Gibraltar	-1.3	1	1.3	**10.8**	-1.6	-7	2.1	**17.5**
	Tarifa	-1	-1	1.1	**6.9**	-2	-2	2.1	**13.1**
	Mean	0.9± 0.4	-0.5± 0.9	0.6± 0.3	**5.2**	1.5± 0.5	3.8± 2.1	1.2± 0.5	**10.2**
K1	Algeciras	0.82	5	0.9	**45.0**	0.78	-2	0.8	**40.0**
	Ceuta	1.8	6	1.8	**45.0**	1.3	0	1.3	**32.5**
	Gibraltar	0.65	3	0.7	**35.0**	0.54	-4	0.6	**30.0**
	Tarifa	0.39	0	0.4	**13.3**	0.59	-12	0.8	**26.7**
	Mean	-0.9± 0.5	-3.4± 2.3	0.7± 0.4	**19.5**	-0.8± 0.3	4.4± 4.7	0.6± 0.3	**19.5**
O1	Algeciras	0.33	-35	0.7	**70**	-0.0041	-27	0.4	**40**
	Ceuta	2.1	-10	2.2	**110**	1.3	-8	1.3	**65**
	Gibraltar	0.11	-35	0.6	**60**	-0.056	-30	0.4	**40**
	Tarifa	**-0.032**	**-21**	**0.2**	**-**	-0.27	-60	0.4	**-**
	Mean	-0.6± 0.9	25.4± 10.4	0.6± 0.6	**42.0**	-0.2± 0.6	31.2± 18.5	0.4± 0.4	**47.6**

Table 3 : Model performance statistics for the main barotropic tidal components (M2, S2, K1, O1) in $\boldsymbol{R_{NBQ}}$ *and the forcing simulation in comparison to tidal gauges (Algeciras + Ceuta). dA = mean amplitude biais; dG = mean phase bias; | | dE| | = mean combined bias; | | dE| | /A = mean relative bias.*

=> Comparaison CROCO-MITgcm : Meilleure représentation des semi-diurnes mais moins bonne représentation des diurnes sauf à Tarifa : explication possible : Pression Atm? Extension du domaine? Amplitude très faibles donc plus sensible aux différences de topo?

Simulation		R_H				RNBQ			
Tidal compo-nents	Tidal gauges	dA (cm)	dG (°)	| | dE| | (cm)	| | **dE**| | /**A** (%)	dA (cm)	dG (°)	| | dE| | (cm)	| | **dE**| | /**A** (%)
M2	Algeciras	-3.7	-3	3.9	**12.2**	-3.8	-2	4.0	**12.5**
	Ceuta	-4	4	4.4	**14.7**	-4.4	3	4.7	**15.7**

continued on next page

continued from previous page

	Gibraltar	-6.4	-1	6.4	**20.0**	-6.5	0	6.5	**20.3**
	Tarifa	-5.7	-1	5.8	**13.8**	-5.6	-1	5.7	**13.6**
	mean	5.0± 1.1	0.2± 2.3	3.5± 1.1	**11.5**	5.1± 1.0	0.1± 2.1	3.6± 1.0	**11.8**
S2	Algeciras	0.16	1	0.2	**1.7**	-0.14	1	0.3	**2.5**
	Ceuta	-0.55	3	0.7	**6.4**	-0.95	1	1.0	**9.1**
	Gibraltar	-1.1	0	1.1	**9.2**	-1.3	1	1.3	**10.8**
	Tarifa	-1	-1	1.0	**6.3**	-1	-1	1.1	**6.9**
	mean	0.6± 0.5	-0.7± 1.2	0.5± 0.4	**4.5**	0.9± 0.4	-0.5± 0.9	0.6± 0.3	**5.2**
K1	Algeciras	0.79	2	0.8	**40.0**	0.82	5	0.9	**45.0**
	Ceuta	1.6	6	1.7	**42.5**	1.8	6	1.8	**45.0**
	Gibraltar	0.61	0	0.6	**30.0**	0.65	3	0.7	**35.0**
	Tarifa	0.42	-3	0.4	**13.3**	0.39	0	0.4	**13.3**
	mean	-0.9± 0.5	-3.4± 2.3	0.7± 0.4	**19.5**	-0.9± 0.5	-3.4± 2.3	0.7± 0.4	**19.5**
O1	Algeciras	0.3	-36	0.7	**70**	0.33	-35	0.7	**70**
	Ceuta	2.3	-14	2.4	**120**	2.1	-10	2.2	**110**
	Gibraltar	-0.029	-39	0.6	**60**	0.11	-35	0.6	**60**
	Tarifa	-0.065	-19	0.2	-	-0.032	-21	0.2	**-**
	mean	-0.7± 1	26.9± 10.7	0.7± 0.6	**43.4**	-0.6± 0.9	25.4± 10.4	0.6± 0.6	**42.0**

Table 4 : Model performance statistics for the main barotropic tidal components (M2, S2, K1, O1) in $\boldsymbol{R_{NBQ}}$ & $\boldsymbol{R_H}$ *in comparison to tidal gauges (Algeciras + Ceuta). dA = mean amplitude biais; dG = mean phase bias;* $|\,|\,dE|\,|$ *= mean combined bias;* $|\,|\,dE|\,|\,/A$ *= mean relative bias.*

=> Comparaison Hydro vs NBQ : difficile de conclure

=> Même score en Hydro pour les diurnes?

0.0.3 The internal fine-scale processes

We focus on internal fine-scale processes generated by tidal flow. In this area, they are subject to a strong neap-spring tidal variability. Hence, to study their dynamic, we distinct three different regime of tidal forcing during the modelled time period (Figure 3):

- a week tidal forcing when the minimal barotropic velocity above CS crest during the tidal outflow is superior to -0.5 m/s (green curve)
- a moderate tidal forcing when the minimal barotropic velocity above CS crest during the tidal outflow is inferior to -0.5 m/s and superior to -1.5 m/s (blue curve)
- a strong tidal forcing when the minimal barotropic velocity above CS crest during the tidal outflow is inferior to -1.5 m/s (red curve)

During the modelled time period of one month, the moderate tidal forcing is the dominant regime.

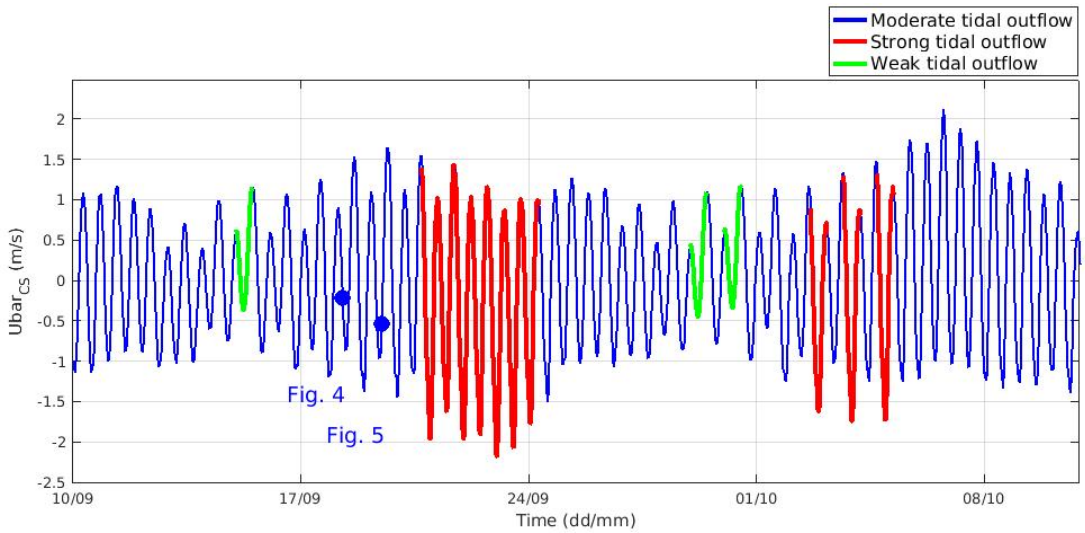

Figure 3 : Barotropic velocity above CS crest. The colored curves differentiate the three different tidal regimes : green curves - weak tidal forcing, blue curves - moderate tidal forcing and red curves - strong tidal forcing. The circle markers indicate the acquisition date of the high-resolution satellite images on figure 4 and 5.

0.0.3.1 Comparison to high-resolution satellite images

An effective procedure to trace the evolution of the internal or baroclinic field consists of monitoring the spatial gradient of surface velocity. The superposition of baroclinic and barotropic currents gives rise to areas of strong horizontal convergence/divergence of the flow characterized by short-scale surface roughness which can be captured by SARs

[Alpers, 1985] and MSI- Multispectral Imager. This allows for the identification of baroclinic structures such as internal hydraulic jumps or internal propagating internal waves through the observation of the ocean surface.

Multiple SAR and RGB images have been acquired from Sentinel-1 and sentinel-2 satellites during the modelled time period (10/09/2017 - 10/10/2017). We focus on two particular satellite images acquired both in moderate regime but at different phases of the tidal cycle:
- a SAR image acquired on the 18/09/2017 – 06:27:42 at the end of the tidal cycle
- a RGB image acquired the 19/09/2017 – 11:18:00 just after the tidal maximal outflow.

The SAR image was taken at the end of a moderate tidal cycle when the well-known train of ISWs propagating eastward reaches the bay of Gibraltar (Figure 4 - Left panel). The train of ISWs on the SAR image is composed at least of 4 distinct solitary waves. On this particular SAR image, a second feature is identifiable as a westward propagating internal wave in Tangier Bassin. The origin of these westward propagating internal waves will be discuss in section 3.3.

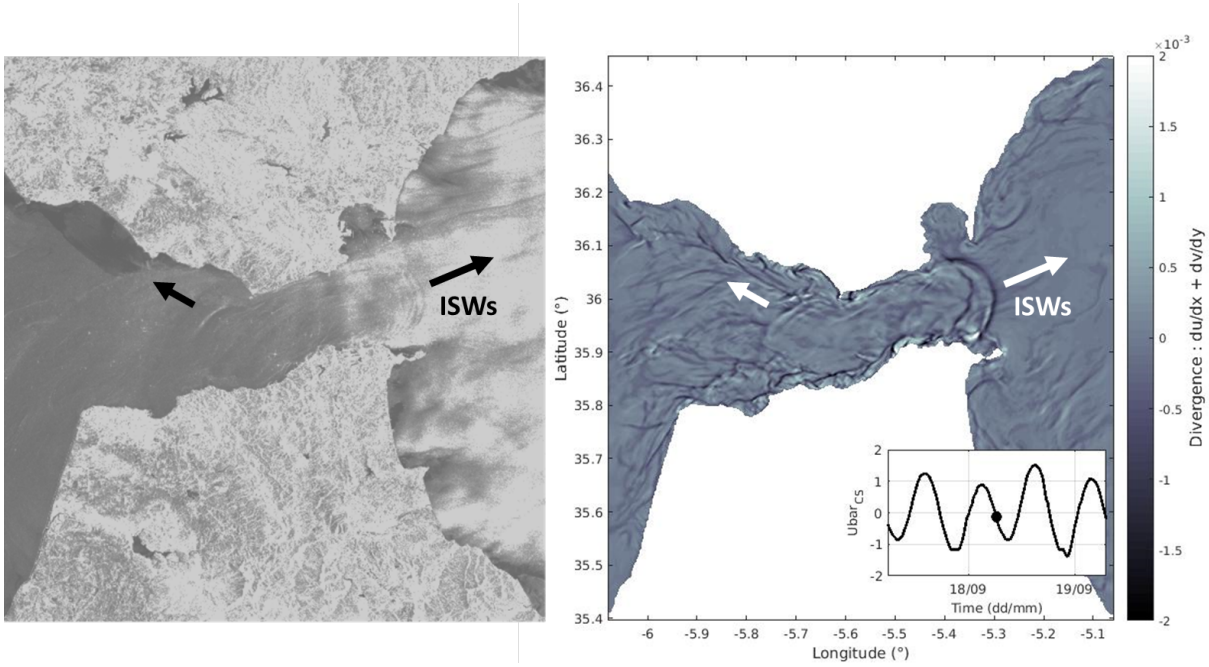

Figure 4 : Left – Sentinel-1 Synthetic Aperture Radar (SAR) image acquired on the 18/09/2017 – 06:27:42 and processed by ESA. Right - Divergence of the flow in ***SimNBQ*** *the 18/09/2017 – 06:25:00 after a moderate tidal outflow.*

The RGB image (Figure 5 - Upper panel) was taken just after the maximum of a moderate tidal outflow when hydraulic jumps are presumably formed in the lee-side of the main sill. On this particular RGB image, instead of the expected single wavefront, two distinct fronts can be observed in CS area : one downstream of CS extending all across the strait and another one upstream of CS more localized. At this phase of the tidal cycle, the train of ISWs generated during the previous tidal outflow is still propagating eastward inside the Alboran sea and is composed by a larger number of solitary waves than in the above SAR image. Near the peninsula de Almina, we can observe a small signature of a strong

horizontal gradient, not consistent with the ISWs propagation, possibly associated to a frontal area. The hypothetical processes responsible for this signature will be discuss in section 3.4.

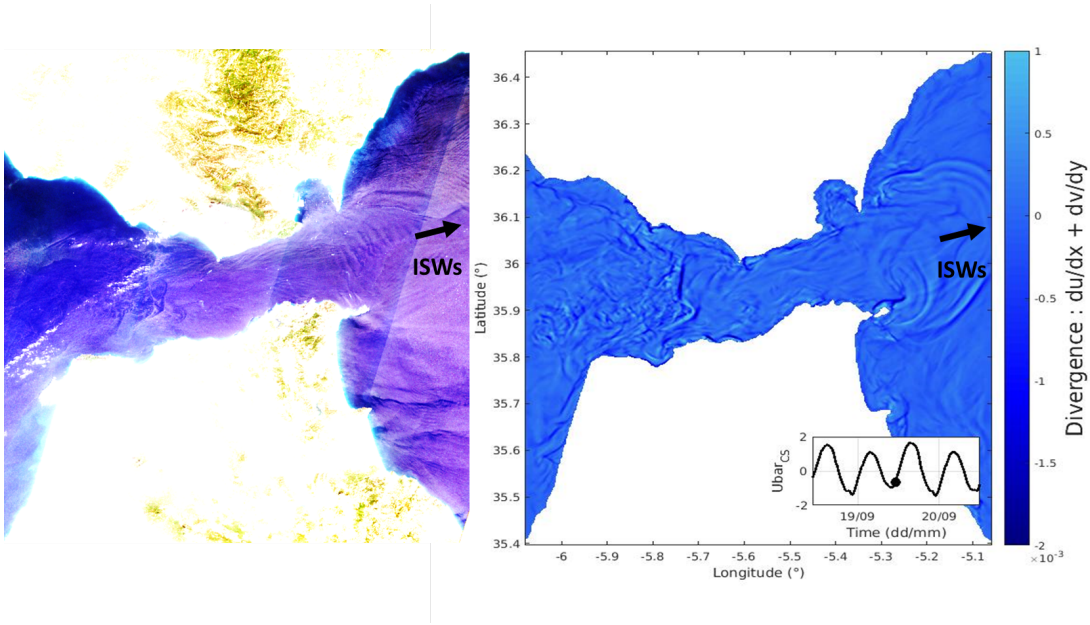

*Figure 5 : Upper - BOA reflectance image (RGB composites) on 19/09/2017 11:18:08, re-processed from Level-2A product for Sentinel-2A/MSI instrument distributed by ESA – Lower - Sea suface elevation output of **SimNBQ**, the 19/09/2017 – 11:18:00 at a moderate tidal outflow.*

Comparaison image SAT - modèle :
∗ Résolution image sat 10m vs résolution du modèle 220 m∗

ISWs
=> bonne position du train = bonne vitesse de propagation
=> Sous-estimation du nombre de soliton dans le train : résolution insuffisante?
=> Déformation de l'arc de cercle du soliton lié au "frottement" à la côte "sous-estimé" dans le modè

Westward propagating waves :
=> bonne position = bonne vitesse de propagation
=> bonne orientation
=> même asymétrie avec un gradient max dans la partie centre-nord du détroit

HJs
=> Dans la simu : les ressauts ont déjà étaient relâché (ubar_cs<c1), on visualise la propagation des
=> Il semble qu'il y est un léger déphasage de la marée barotrope au dessus de CS...

Peninsula de Almina

=> même position du gradient

0.0.3.2 Hydraulic jumps dynamic

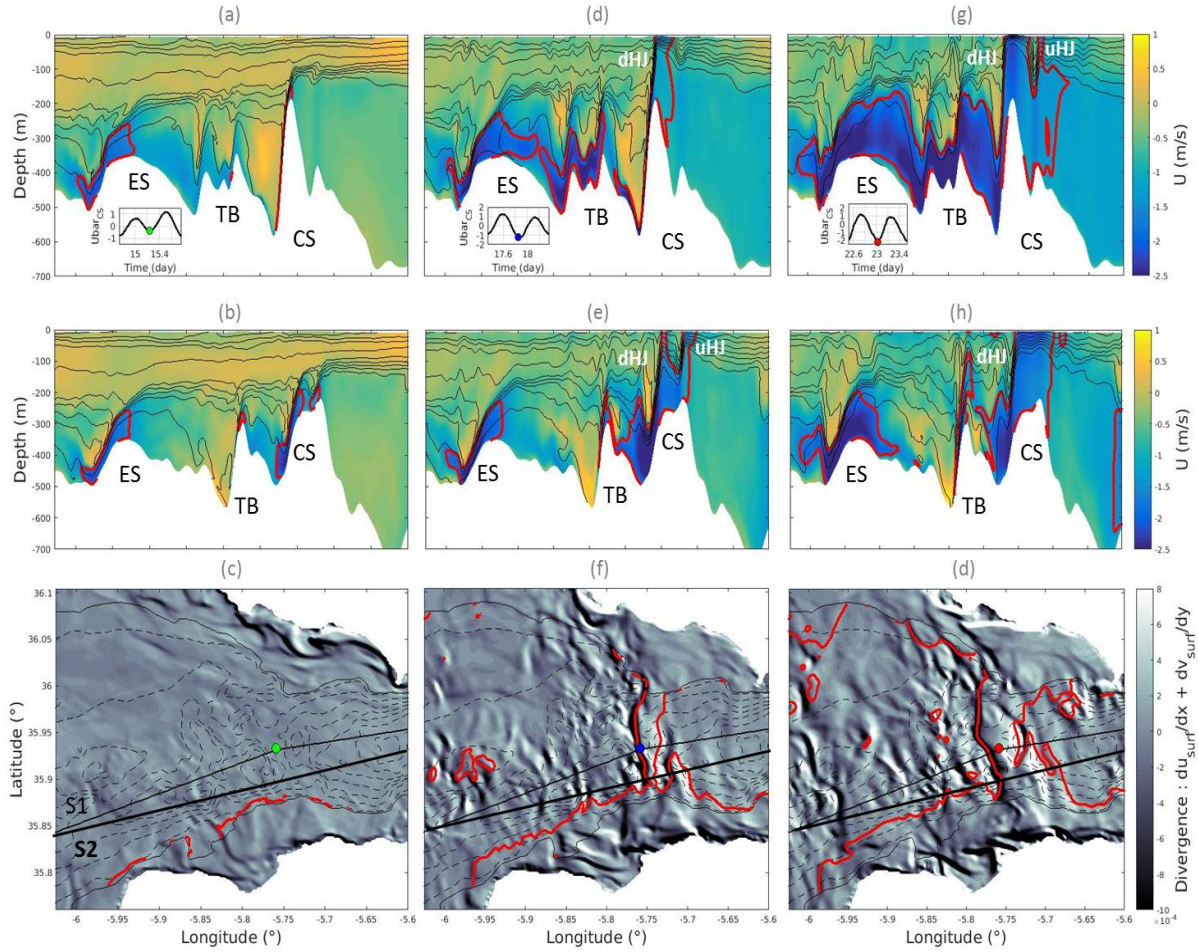

*Figure 6 : Lower pannels - Divergence of the flow in **R0** at the maximum of a weak tidal outflow (c), a moderate tidal outflow (f) and a strong tidal outflow (d). The black line locates the vertical section 1 (S1) and section 2 (S2). Middle pannels - Section 2 (S2) of the horizontal velocity field in **R0** at the maximum of a weak tidal outflow (b), a moderate tidal outflow (e) and a strong tidal outflow (h). Upper pannels - Section 1 (S1) of the horizontal velocity field in **R0** at the maximum of a weak tidal outflow (a), a moderate*

tidal outflow (d) and a strong tidal outflow (g). Red contour represent supecritical flow area (F1=c1).

Under weak tidal forcing, only a small part of the bottom layer is supercritical above CS crest (partial HC).

Under moderate tidal forcing, strong asymmetry between the north and the south of the strait (due to geographical constriction) :

- one supercritical region above CS crest in the north
- two separated supercritical regions in the south part of the strait

=> Two HJs : one downstream CS extending from the north to the south of the strait and one upstream, formed only in the south part of the strait
The front located downstream (to the west) appears in the image almost as a straight line extending all across the strait, but the one located upstream is confined to the southern half of the section.

Under strong tidal forcing (spring tides), when the outflow is maximal, the south upstream internal bores (located initially around -5.73° of longitude) are swept down to the lee side of the sill (around -5.76° of longitude) , and in the south part of the strait, the flow acquires the hydraulic configuration of a pure approach-controlled state, with only one supercritical region extending from the upstream control section to a few hundred meters downstream (CS crest).
However in the middle part of the strait, there is two separated supercritical regions in the surface layer one above CS and a second one upstream CS crest. On figure$* * *$, in the middle of the strait, we observe the signature of a downstream & a upstream HJs.
=> fusion des ressauts aux sud du détroit en vives-eaux : même résultats que Garrido avec le MITgcm : Ref: http://oceano.uma.es/pdfpub/2011Numerical% 20.pdf

0.0.3.3 ISWs formation: a strong neap-spring tide variability

During moderate tides, two internal hydraulic jumps are formed above Camarinal sill (CS) at maximum tidal ouflow: one upstream (uHJ) and another dowstream (dHJ) of the sill (« uncontrolled » flow state[10]). When the tidal flow reverses, the hydraulic jumps are released and lead to the eastward propagation of an/ two internal bore (IB). $* * *$ one propagating to the south-east and one $* * * .$ $* *$ fusion des deux bores$* * * .$ It is then subject to multiple reflexions (rW) in Tarrifa Narrows and degenerates into solitary waves (ISWs).
=> generation of an IB downstream of CS

However, during weak neap-tides; the favourable hydraulic conditions for the generation

of lee waves (LWs) in the lee-side of Camarinal sill inhibit the internal bore generation (boiling water phenomena[11]) . => no generation of IB

After strong tidal outflow, two IB are generated one downstream and one upstream of CS. The large downstream bore propagates faster and $* * *$.

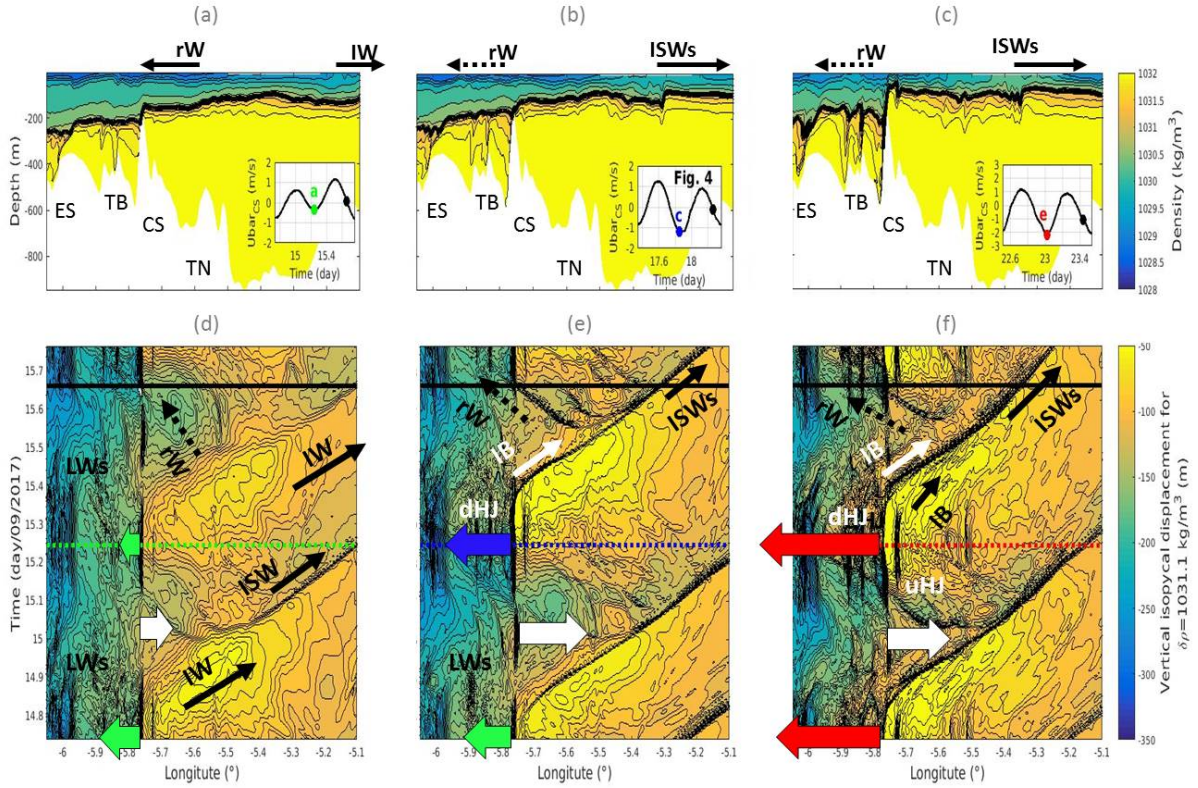

*Figure 7: Upper panels - Section 1 of the density field in **R0** after a weak tidal outflow (a), a moderate tidal outflow (b) and a strong tidal outflow (c). Lower panels - Space-time diagram of the vertical isopycnal displacement for ρ =1031.1 kg/m3 (bold black line on the upper panels) along the section 1 during two weak tidal cycle (a), a moderate and a weak tidal cycle (b) and two strong tidal cycle (c). The white arrows represent the mean tidal inflow above Camarinal sill whereas colored arrows represent the mean tidal outflow above Camarinal sill (green for weak, blue for moderate and red for strong). Horizontal black lines locate temporally the vertical section of the density field (upper panels) whereas colored dotted lines locate temporally the maximum of the previous tidal outflow (section 1 on Fig. 6).*